

Supporting information

One-pot synthesis of redox-triggered biodegradable hybrid nanocapsules with disulfide-bridged silsesquioxane framework for promising drug delivery

Mengyun Zhou,^a Xin Du,^{*a} Weike Li,^a Xiaoyu Li,^b Hongwei Huang,^c Qingliang Liao,^d Bingyang Shi,^e Xueji Zhang^a and Meiqin Zhang^{*a}

^a Research Center for Bioengineering and Sensing Technology, Beijing Key Laboratory for Bioengineering and Sensing Technology, School of Chemistry and Biological Engineering, University of Science & Technology Beijing, Beijing 100083, P. R. China

*E-mail: duxin@ustb.edu.cn; zhangmeiqin@ustb.edu.cn

^b National Engineering Laboratory for Hydrometallurgical Cleaner Production Technology, State Key Laboratory of Biochemical Engineering, Key Laboratory of Green Process and Engineering, Institute of Process Engineering, Chinese Academic of Sciences, Beijing 100190, China

^c School of Materials Science and Technology,
China University of Geosciences, Beijing 100083, China

^d State Key Laboratory for Advanced Metals and Materials, School of Materials Science and Engineering, Beijing Municipal Key Laboratory of New Energy Materials and Technologies, University of Science and Technology Beijing, Beijing 100083, China

^e Faculty of Medicine and Health Sciences, Macquarie University, Sydney, New South Wales 2109, Australia.

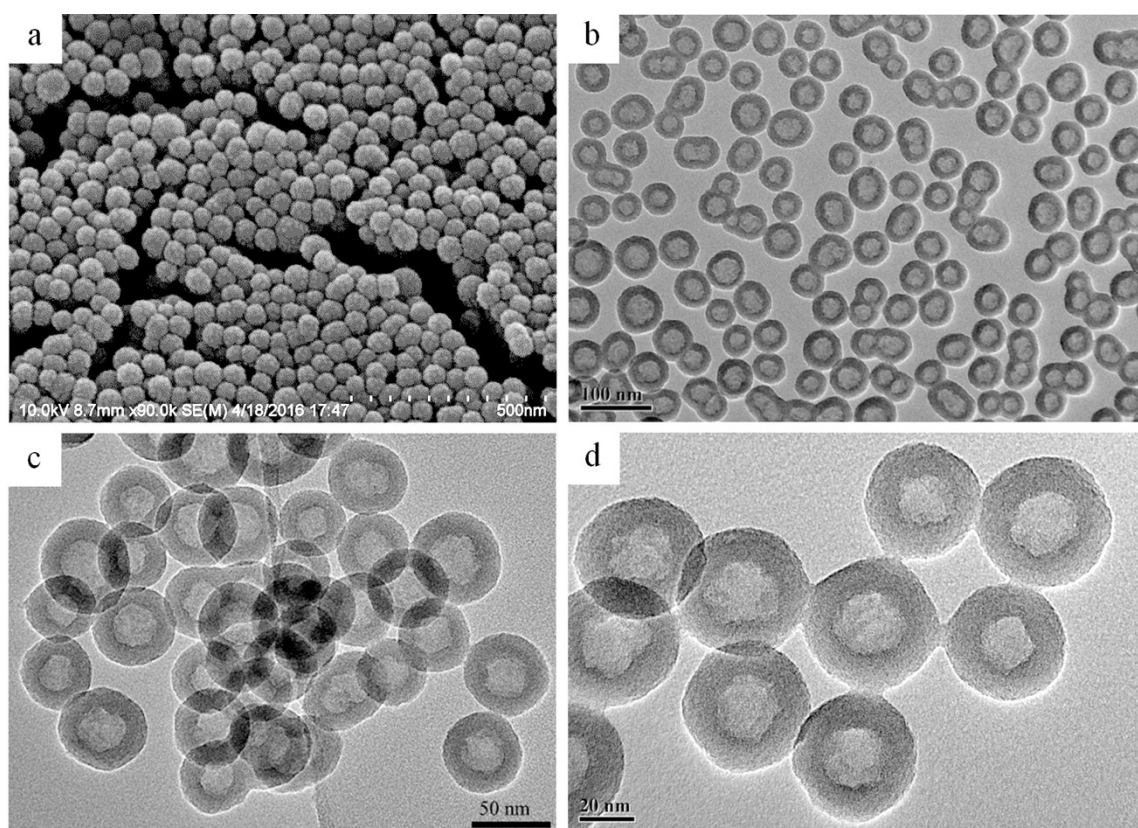


Figure S1. SEM (a) and TEM (b-d) images of uniform hollow silica nanospheres (HSNs) by using TEOS as silicon source. The particle size is about 50~60 nm, while the size of hollow cavity is about 20~30 nm.

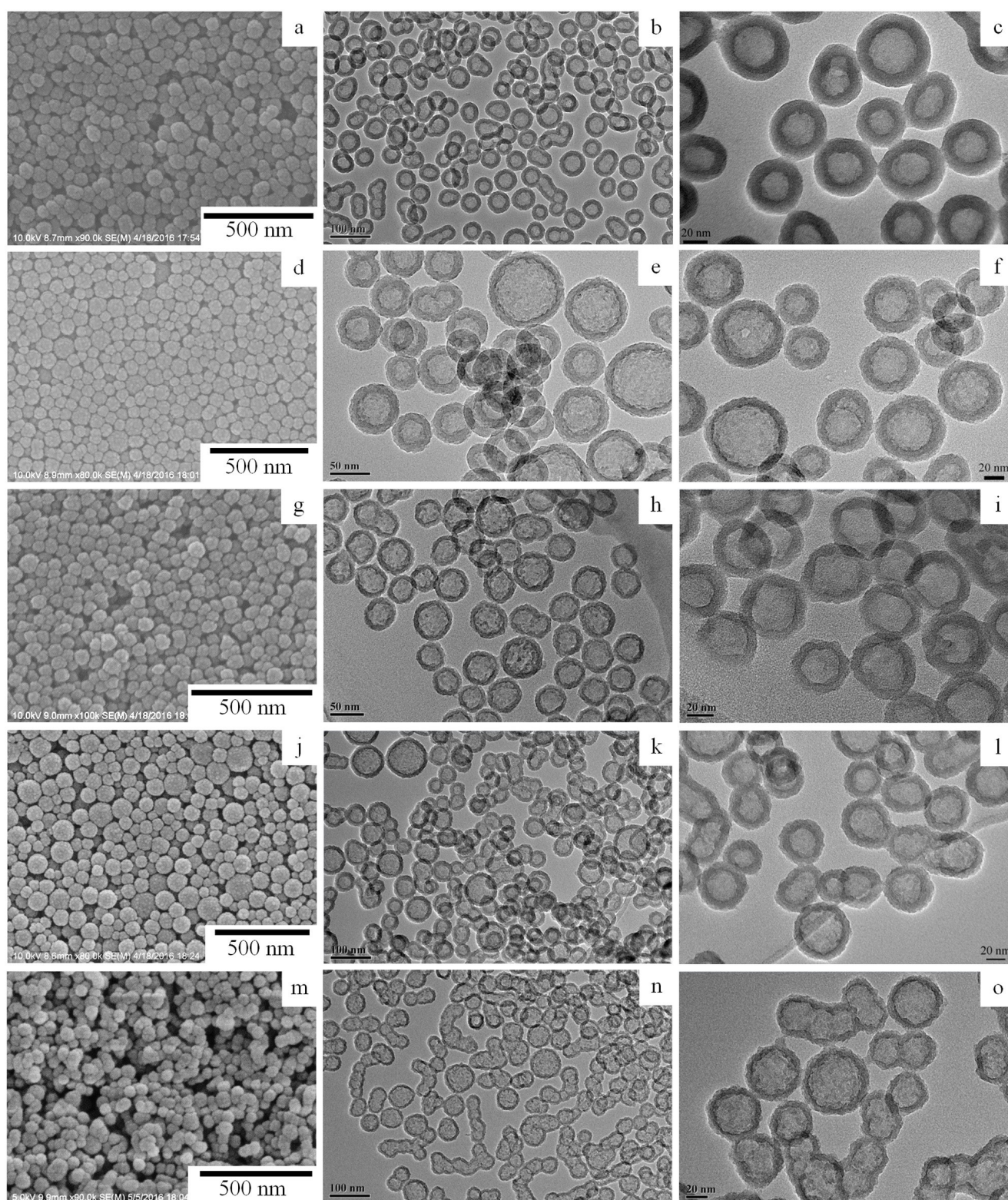


Figure S2. SEM and TEM images of HSNs fabricated under varied amount of TEOS (mL) and BTEPDS-2S (mL): (a-c) 1.3 and 0.2, (d-f) 1.1 and 0.4, (g-i) 0.9 and 0.6, (j-l) 0.75 and 0.75, and (m-o) 0.6 and 0.9, respectively.

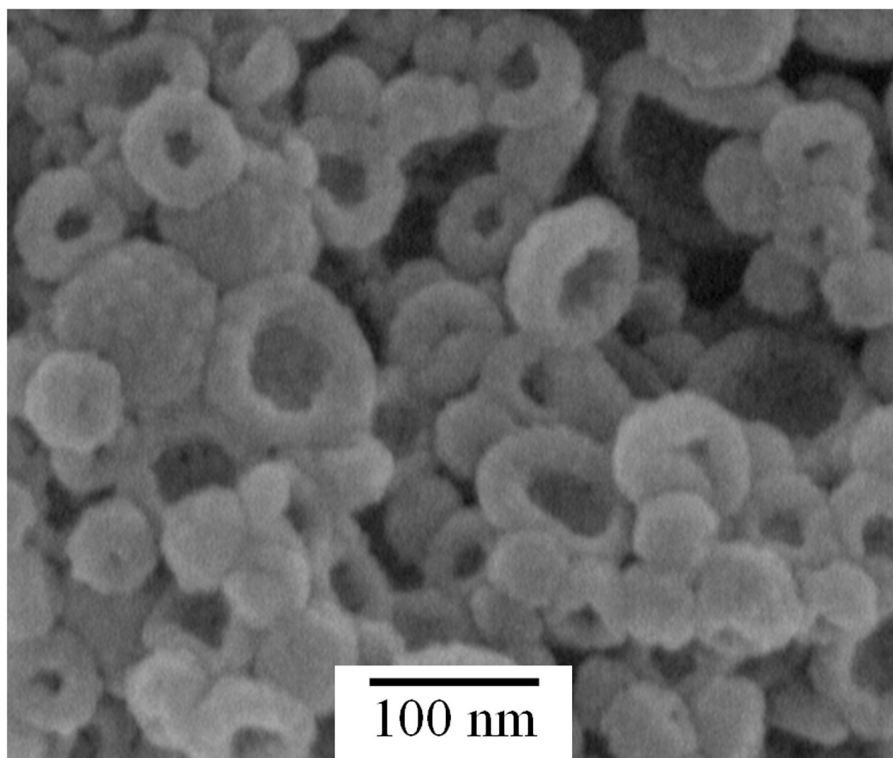


Figure S3. SEM image of HSNs-4S fabricated under varied amount of 0.9 mL of TEOS and 0.6 mL of BTEPTS-4S, followed by the treatment of ammonia solution for 20 min.

20 min of treatment time is longer than that (5 min) for intact nanocapsules with enlarged pores in the shells. This long time treatment results in the rupture of nanocapsules due to excessive etching.

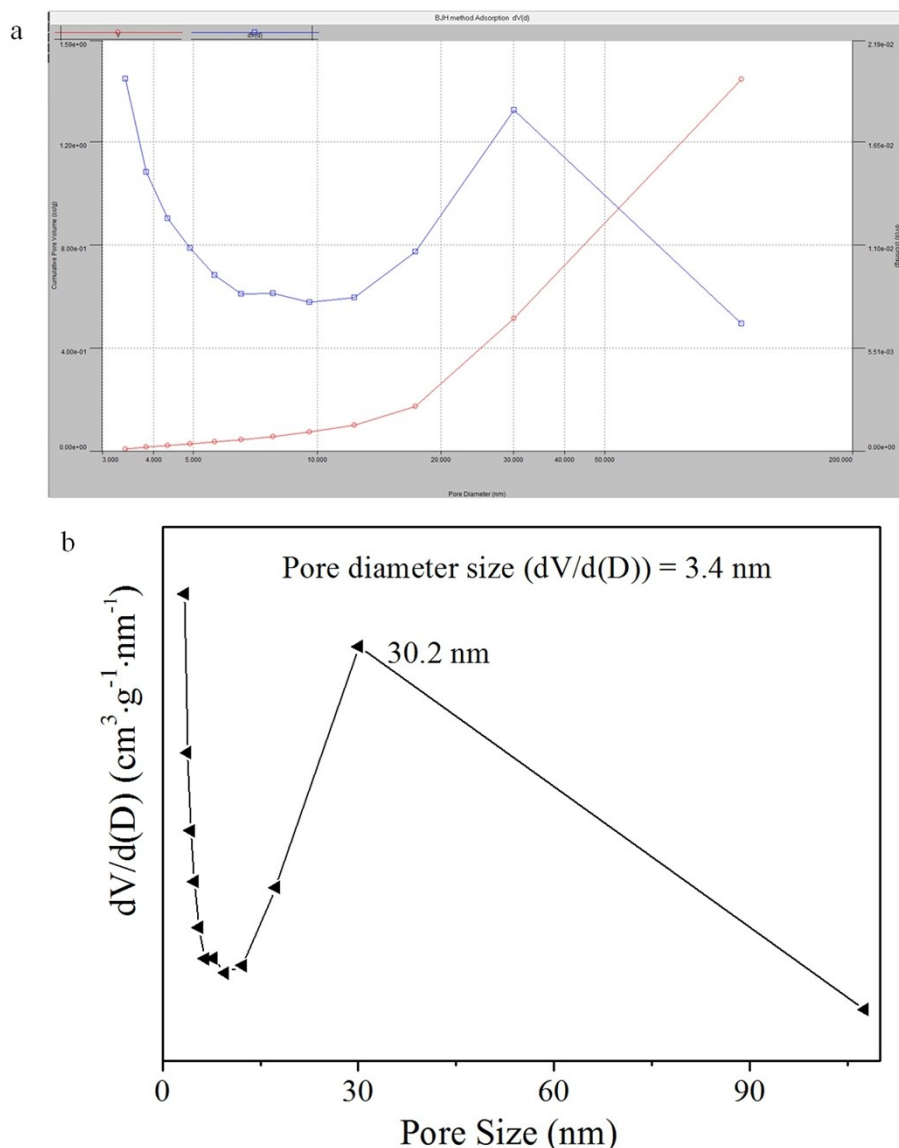


Figure S4. BJH pore size distribution curve obtained from adsorption branch of the isotherm of the etched HSNs-4S: (a) image is directly cut from ASiQwin software; (b) image is plotted by Origin software. The pore size distribution curve exhibits a broad peak centered at 30.2 nm, which should be the size of hollow cavity. Pore diameter size ($dV/d(D)$) from BJH adsorption summary is 3.4 nm.

Due to invisible pore size distribution between 0~3.5 nm from BJH method, QSDFT method was employed to obtain pore size distribution curve. In the QSDFT pore size distribution curve, one strong peak centered at 3.6 nm should be the size of disordered mesopores in the shell, while two peaks centered at 20.2 and 27.8 nm should be sizes of hollow cavities.

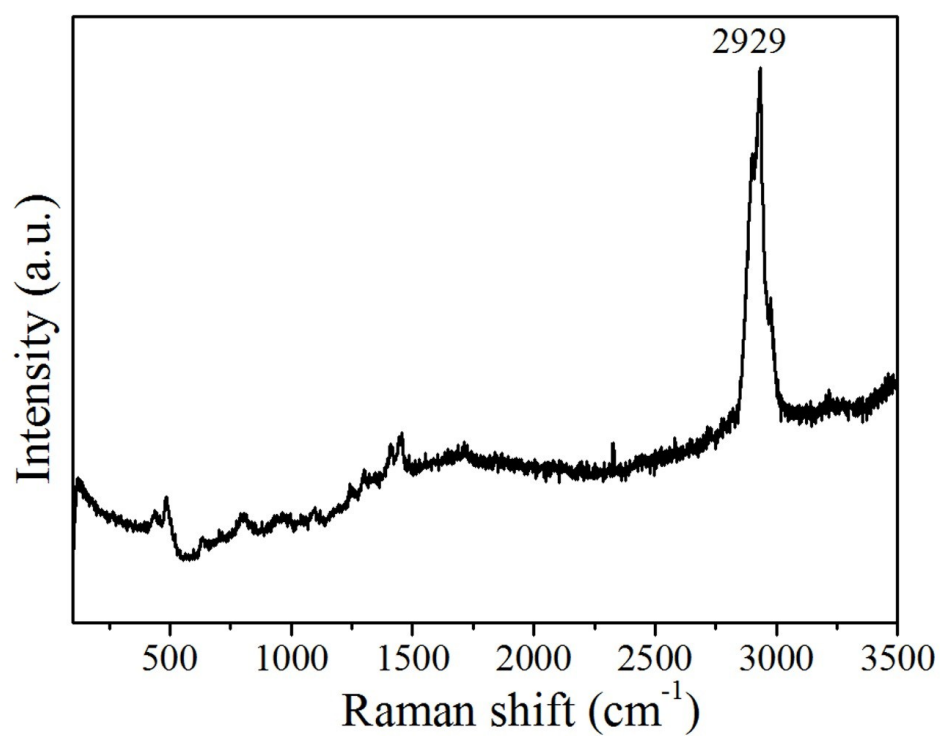


Figure S5. Raman spectrum (c), EDX spectrum (d), and TEM (e) and element mapping images (f-h) of the etched HSNs-4S fabricated with 0.9 mL of TEOS and 0.6 mL of BTEPTS-4S, followed by the treatment of ammonia solution.

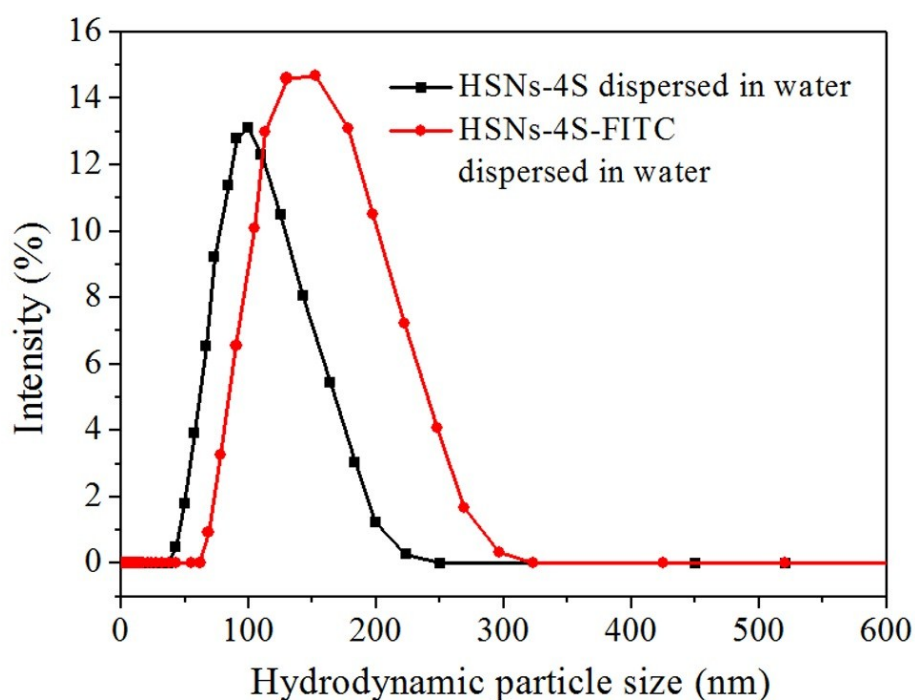


Figure S6. Distribution curves of hydrodynamic particle sizes of HSNs-4S and HSNs-4S-FITC dispersed in water.

As shown in **Figure S6**, the mean hydrodynamic particle sizes of HSNs-4S and HSNs-4S-FITC dispersed in water are ca. 112 nm and 172 nm, respectively. FITC introduction causes the increase of hydrodynamic particle size from ca. 112 to 172 nm. In addition, after PEG modification, their hydrodynamic particle sizes increased from ca. 172 to 185 nm.

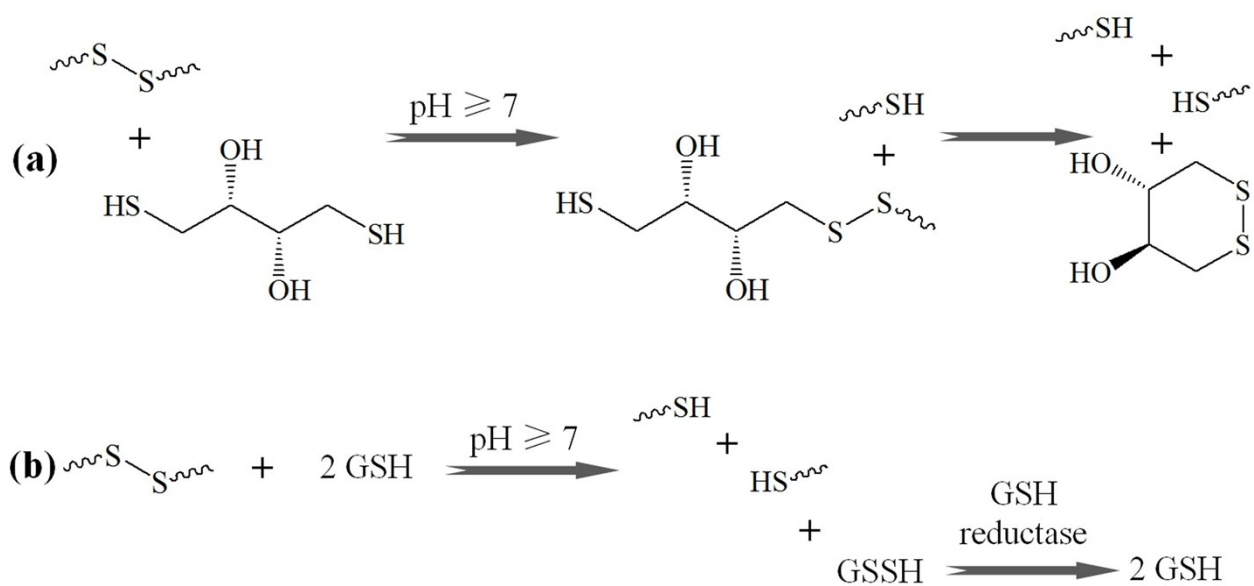


Figure S7. Molecular formulas of chemical reactions between disulfide bond (-S-S-) and DTT (a), and -S-S- and GSH, then with GSH reductase (b).

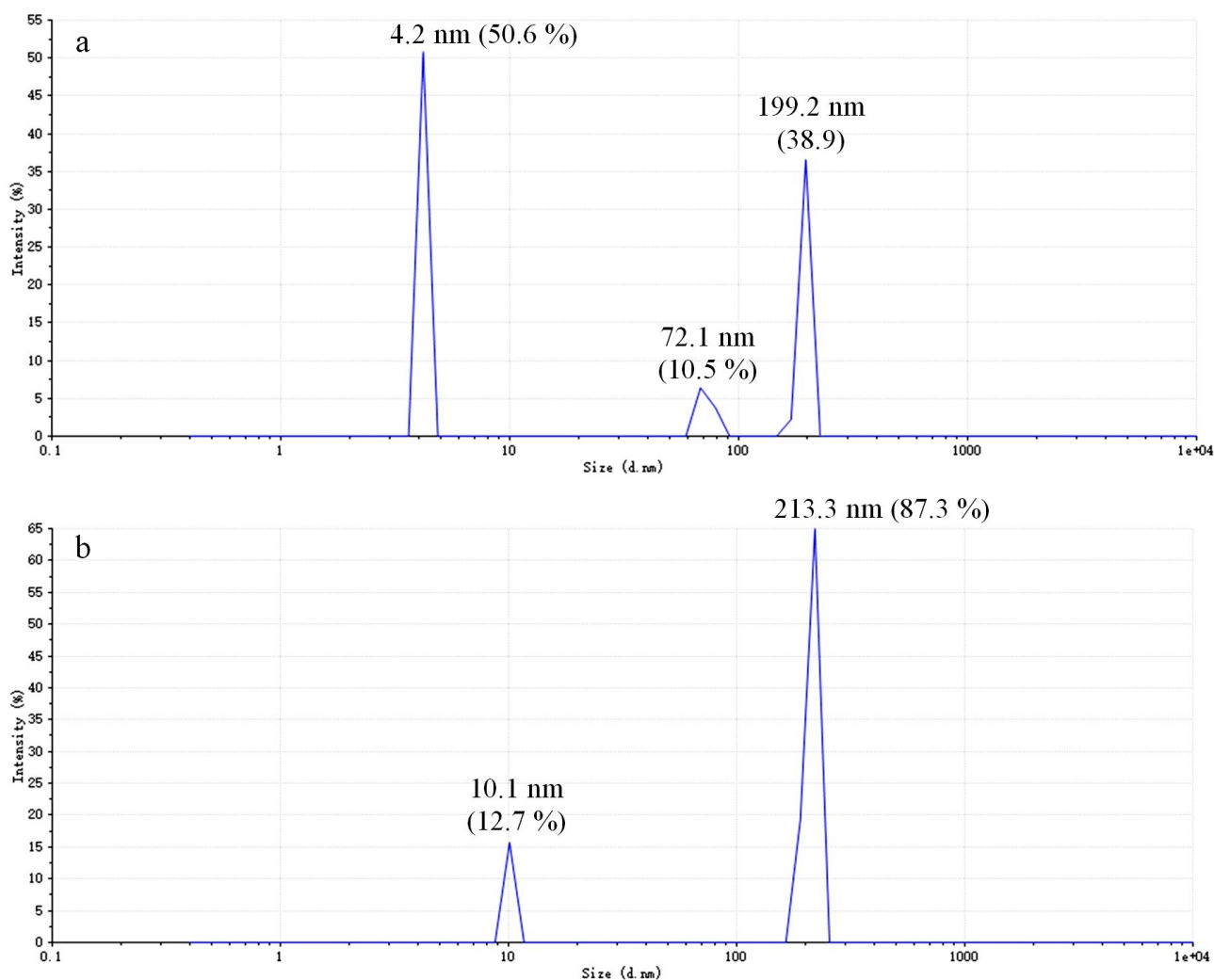


Figure S8. Distribution curves of hydrodynamic particle sizes of HSNs-4S-FITC/PEG stirred in 5 mM of DTT (a) and 10 mM of GSH (b) at 37 °C for 8 days.

After HSNs-4S-FITC/PEG were stirred in 5 mM of DTT at 37 °C (a), the hydrodynamic particle sizes of biodegraded products are 4.2 (50.6 %), 72.1 (10.5 %) and 199.2 (38.9 %) nm, while the hydrodynamic particle sizes of biodegraded products are 10.1 (12.7 %) and 213.3 (87.3 %) nm after they were stirred in 10 mM of GSH (b) for 8 days. The result is largely agreeable with those from SEM and TEM images. The reducing capacity of 5 mM DTT is higher than that of 10 mM GSH. These results also show that DTT or GSH cannot break down all the NPs, thus the biodegradation capacity of HSNs-4S-FITC/PEG need to be improved for efficient excretion.

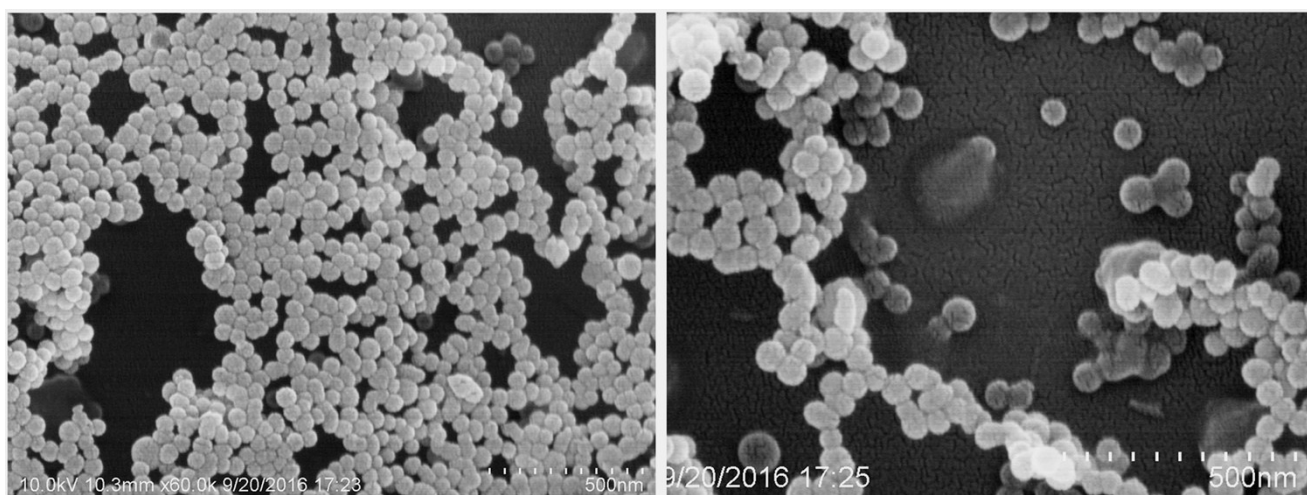


Figure S9. SEM images of HSNs after stirred in DDT (5 mM) solution for 8 days.

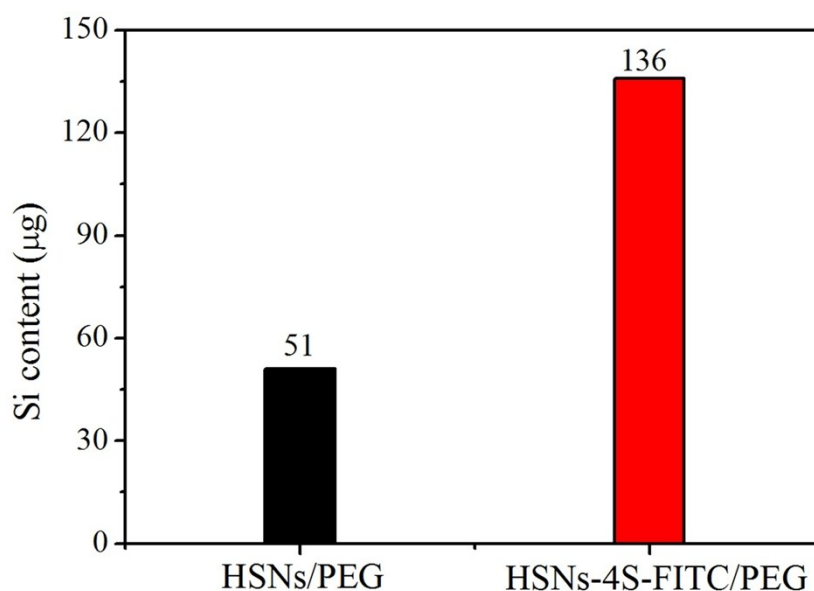


Figure S10. Si contents in different cell culture mediums of A549 cells treated with HSNs-PEG or HSNs-4S-FITC/PEG after incubation for 48 h, which are measured by ICP-AES.

Si element should come from the excreted silica species because most particles without interaction with cells had been removed by washing with PBS three times. Si content in cell culture medium of A549 cells treated with HSNs-4S-FITC/PEG is ca. 2.7 times as large as that treated with HSNs/PEG. More excreted Si species result from the formation of smaller fragments, which facilitates the excretion from cells. The result suggests intracellular GSH-trigger biodegradation of HSNs-4S-FITC/PEG.